

JOURNAL OF BIOMEDICINE AND TRANSLATIONAL RESEARCH

Available online at JBTR website: <https://jbtr.fk.undip.ac.id>

Copyright©2023 by Faculty of Medicine Universitas Diponegoro, Indonesian Society of Human Genetics and Indonesian Society of Internal Medicine

Original Research Article

Comparative Analysis of Kidney Histomorphometry Utilizing Two Distinct Image Processing Software

Ageng Brahmadhi^{1*}, Ira Citra Ningrom²

¹Histology Laboratory, Faculty of Medicine, Universitas Muhammadiyah Purwokerto, Indonesia

²Patology Anatomy Laboratory, Faculty of Medicine, Universitas Muhammadiyah Purwokerto, Indonesia

Article Info

History

Received: 08 Jun 2023

Accepted: 21 Nov 2023

Available: 31 Dec 2023

Abstract

Background: Histopathological examination is critical to evaluate tissue condition. An accurate assessment is necessary for diagnosis establishment. Nowadays, both quantitative and qualitative scoring are enhanced with computer-assisted image analysis to reduce bias. Various software was developed to assist in image analysis. The question of whether the measurement results from one software will be comparable to those from another software may come up, given the wide variety of software options. Nevertheless, this subject is only occasionally discussed.

Objective: This study aimed to compare the measurement results from two open-source software, Fiji and QuPath software in kidney histomorphometry.

Methods: Five histological slides of normal kidney were observed. Selected histological structures, including the renal corpuscle area, glomerular area, Bowman space area, inner diameter of proximal, distal, and Henle loop, were measured using QuPath (version 0.3.2) and Fiji (version 1.53c) software. The measurement results from the two software were compared for value differences and agreement analysis.

Results: The renal corpuscle means the area was $12.7 \times 10^3 \mu\text{m}^2$ in QuPath and $12.5 \times 10^3 \mu\text{m}^2$ in Fiji. The glomerular area was $7.8 \times 10^3 \mu\text{m}^2$ for both software. The proximal tubule's inner diameters varied from 18.7 to 150.8 μm . Smaller inner diameters were observed in distal tubules (17.1-80.5 μm) and The Henle loop (15.5-69.6 μm). There was no significant difference in measurement results of particular structures between the compared software (P-value > 0.05). The further confirmational analysis supported the similarity between the two measurement results.

Conclusion: the measurement result of kidney microstructures using QuPath and Fiji were identical.

Keywords: Kidney; Histology; Computer-assisted; Histomorphometry

Permalink/ DOI: <https://doi.org/10.14710/jbtr.v9i3.18554>

INTRODUCTION

Histopathological examination is critical to evaluate the condition of cells, tissues, and organs. An accurate assessment is necessary for diagnosis establishment or determining disease progression. Generally, a histological examination can be performed semi-quantitatively or quantitatively using virtual images and measuring tissue histology parameters.

Both quantitative and qualitative methodologies have advantages and disadvantages. The qualitative diagnosis is based on identifiable morphological changes in the tissue area of interest and requires trained experts

or pathologists.¹ In the semi-quantitative scoring, the qualitative tissue data are converted into numerical data which enables more reliable group comparison.² The semi-quantitative approach is widely used in preclinical and clinical research. However, a decent experimental design and a reliable scoring system are a must in order to enhance reproducibility and limit result bias.²

*Corresponding author:

E-mail: brahmadhi@ump.ac.id
(Ageng Brahmadhi)

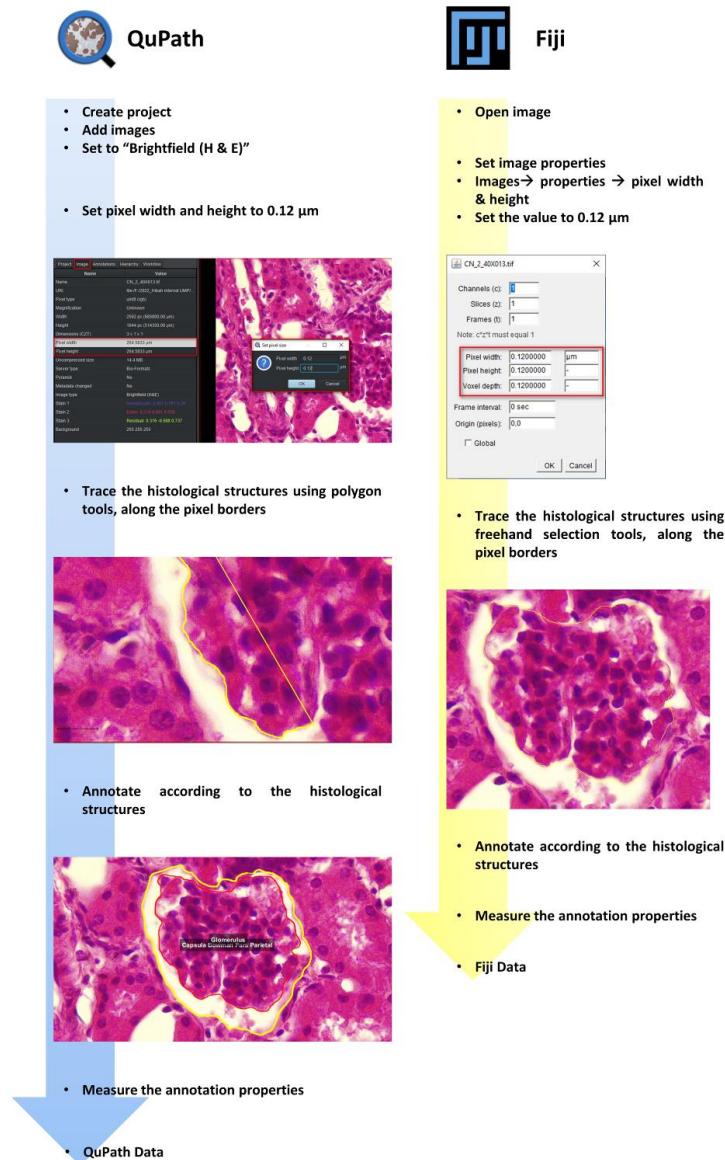


Figure 1. Data acquisition procedures using QuPath and FIJI

Along with technological advancement, either quantitative or qualitative scoring might be enhanced with computer-assisted image analysis to lessen the bias. Various software such as ImageJ,³ Fiji,⁴ QuPath,⁵ Cell profiler analyst,⁶ Advanced cell classifier,⁷ Ilastik,⁸ Cell Cognition Explorer⁹ and many more were developed to assist in image analysis. Typically, two-dimensional sections are used for image analysis, which may produce skewed results. As a result, more advanced methods such as unbiased stereology and whole slide images (WSI) analysis were introduced in histology. Unbiased stereology and WSI analysis provide more reliable data than traditional qualitative and semi-quantitative analysis. However, applying these two methods might not be feasible in some laboratories for several reasons, including method complexity, technology and human resource limitation,⁹ the high initial cost of the scanners, the cost of acquisition, deployment, and operational costs of WSI.¹⁰

Considering the aforementioned limitations, some researchers or laboratories continue to use qualitative or

semi-quantitative tissue assessment. Open-source software is preferable to accommodate the analysis demands. ImageJ was known as one of the pioneers of image analysis software. Along with the technology development, ImageJ was developed further to ImageJ2 and currently known as Fiji. As the next generation of ImageJ, Fiji is equipped with various built-in plug-ins. Another option for open-source software for analysis is QuPath. QuPath is reliable software for digital pathology and is designed to accommodate WSI analysis. However, QuPath is less popular compared to Fiji. The question of whether the measurement results from one software will be comparable to those from another software may come up given the wide variety of software options. To the author's knowledge, this subject is only occasionally discussed. Therefore, this study aims to compare the measurement results from Fiji and QuPath software in kidney histomorphometry.

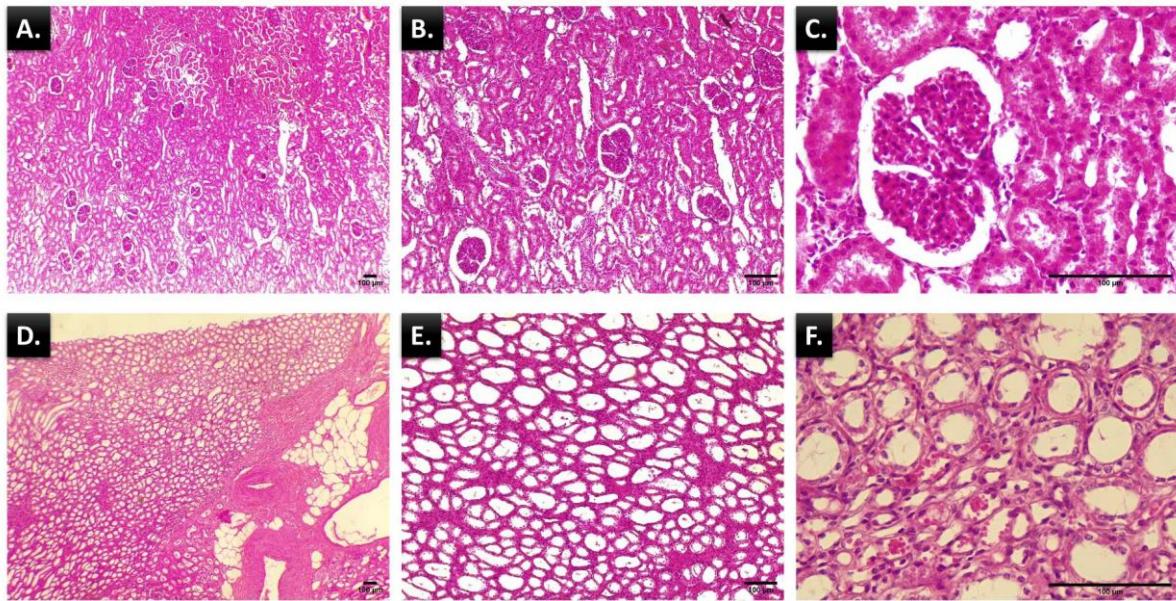


Figure 2. Kidney histological examination in various magnifications. A. Renal cortex at low magnification (4x); B. Renal cortex at medium magnification (10x); C. Renal cortex at high magnification (40x); D, E, and F respectively represent the renal medulla at low, medium, and high magnification.

MATERIALS AND METHODS

Haematoxylin eosin-stained human kidney histological slide was purchased from Ginkomed Taiwan. Five slides (CAT NO H110010) were used in this study. The observation was performed in the cortical and medulla region using Leica DM500. Description of specific tissue characteristics and histological structures in 4x, 10x, and 40x objective magnification were compared.

For histomorphometry analysis, areas containing the renal corpuscle and medulla region were photographed in 40x objective magnification using Leica ocular camera (LCC50E). Leica LAS EZ software was used to obtain calibrated images. The images then proceed further for histomorphometry measurements using open-source software QuPath version 0.3.2 (<https://qupath.github.io/>) and Fiji version 1.53c (<https://fiji.sc/>). Selected histological structures, including the renal corpuscle area, glomerular area, inner diameter of distal tubules, proximal tubules, and Henle loop were measured using QuPath and Fiji (Figure 1). The Bowman space area was calculated by subtracting the renal corpuscle area from glomerular area and expressed in μm^2 . The inner diameter of tubules was stated in μm .

The measurement results from the two software were analysed for data normality using Kolmogorov–Smirnov test and then compared for value differences. The renal corpuscle area, glomerular area and Bowman capsule area were analysed with t-test. The tubules inner diameters were analysed with Mann-Whitney test because the data were not normally distributed. Deming regression and Bland-Altman plot for agreement analysis. P-value < 5% was considered as significant difference between values. The study was approved by the Medical and Health Research Ethics Committee of Faculty of Medicine Universitas Muhammadiyah Purwokerto (No: KEPKK/FK/052/VIII/2023).

RESULTS

Renal histology

Renal tissue examinations were carried out thoroughly, covering the renal cortex to the renal medulla. At low magnification (4x), dark-red tissue parenchyma was seen in the renal cortex. The renal corpuscles were seen as spherical structures, scattered through the cortex. The cortical labyrinth appears as dense parenchyma with a white-colored lumen. However, it is still difficult to distinguish the type of kidney tubules at this magnification. As the magnification increases, the histological structure details become more visible (Figure 2B and C). The glomerulus structure is identified, and the parietal layer of Bowman's capsules can be distinguished from the surrounding tubules. Higher magnification enables renal tubule identification. As shown in Figure 2C, the proximal convoluted tubule with a brush border on its lumen can be distinguished from the distal tubule. A contrasting histological appearance is exhibited in the medulla. In low and medium magnification observation, the renal medulla parenchyma was paler-colored and looser than the cortex (Figure 2D and E). Renal tubules with varying lumen diameters were seen. The collecting tubules, distal tubule, and Henle loop segments appear to predominate in the renal medulla (Figure 2F). However, the proximal tubule is also occasionally found in this region.

Renal structures histomorphometry

Measurement of selected histological structures was performed at 40x objective magnification. In the cortical region, the measurements focused on renal corpuscles, distal tubules, and proximal tubules. The area covered by the parietal layer and renal glomerulus was determined. The area of Bowman space was calculated by subtracting the area contained in the Bowman capsule parietal layer area from the glomerular area. In the medulla region, the measurements were subjected mainly to the inner diameters of the Henle loop.

Table 1. Histomorphometry parameters of kidney microstructures

Histological structures	QuPath	Fiji	<i>p-value</i>
Renal corpuscle area ($\times 10^3 \mu\text{m}^2$)			
Min	6.3	6.3	0.8440 ^{a)}
Max	18.9	18.8	
Mean \pm SD	12.7 \pm 2.9	12.5 \pm 3.0	
Glomerular area ($\times 10^3 \mu\text{m}^2$)			
Min	3.3	3.3	0.9914 ^{a)}
Max	13.3	13.3	
Mean \pm SD	7.8 \pm 2.1	7.8 \pm 2.2	
Bowman space area ($\times 10^3 \mu\text{m}^2$)			
Min	1.7	2.0	0.6539 ^{a)}
Max	8.3	7.8	
Mean \pm SD	4.8 \pm 1.5	4.7 \pm 1.5	
TP inner diameter (μm)			
Min	20.2	18.7	0.8288 ^{b)}
Max	142.4	150.8	
Mean \pm SD	47.7 \pm 25.46	47.5 \pm 26.3	
TD inner diameter (μm)			
Min	17.1	17.8	0.9207 ^{b)}
Max	80.5	79.3	
Mean \pm SD	36.8 \pm 15.0	36.6 \pm 15.0	
HL inner diameter (μm)			
Min	15.7	15.5	0.9322 ^{b)}
Max	68.8	69.6	
Mean \pm SD	35.1 \pm 10.7	34.9 \pm 10.7	

^{a)} *p-values* were obtained from independent *T-test*

^{b)} *p-values* were obtained from Mann-Whitney test

TP: Proximal tubule; TD: Distal tubule; HL: Henle loop.

The measurement showed that the renal corpuscle means areas were $12.7\pm 2.9 \times 10^3 \mu\text{m}^2$ and $12.5\pm 3.0 \times 10^3 \mu\text{m}^2$ for QuPath and Fiji respectively. The glomerular area was $7.8\pm 2.1 \times 10^3 \mu\text{m}^2$ for QuPath and $7.8\pm 2.2 \times 10^3 \mu\text{m}^2$ for Fiji. The calculated mean Bowman space area was $4.8\pm 1.5 \times 10^3 \mu\text{m}^2$ and $4.7\pm 1.5 \times 10^3 \mu\text{m}^2$ for QuPath and Fiji respectively. The T-test showed there was no difference in the measurement from both software (*p-value* > 0.05) (Table 1).

The detailed values of renal tubules' inner diameters are shown in Table 1. Based on our examination using two software, the inner diameter of the proximal tubule ranged from 18.7-150.8 μm . The distal tubules' inner diameter was smaller compared to the proximal tubule, ranging from 17.1-80.5 μm . The Henle loop had the smallest diameter among the other kidney tubules, in the range of 15.5-69.6 μm . From the renal tubule measurements, we also did not find any statistical differences between the two software measurement results (*p-value* > 0.05).

To further confirmed that the measurement from QuPath and Fiji were identical. We analysed the quantification results using Deming regression and the Bland-Altman plot. The Deming regression exhibited linear correlation for quantification of renal corpuscle area (Figure 3A), glomerular area (Figure 3B), and Bowman space area (Figure 3C) in both software. In addition, Pearson's rho values were beyond 0.979 (Figure 3A-C, right panel). The Bland-Altman plot showed most of the measurement values from both software were within the lower and upper limits of agreements. Only a small percentage of values were outside the limit of the agreements range. The off-limit values were 4% for the value of the renal corpuscle area and 8% for either the glomerular or Bowman capsule area value (Figure 3A-C, left panel).

The correlation and linearity from two measurements were also demonstrated for the values of the inner diameter of renal tubules. Pearson's rho values greater than 0.995 was obtained for the distal tubule (Figure 4A) and proximal tubule (Figure 4B). For Henle loop inner diameter, the lower Pearson's rho value was obtained (*r* = 0.880) (Figure 4C). The majority of paired data were within the lower and upper limits of agreement of the Bland-Altman plot. However, we observed 4% off limit values in the distal tubule (Figure 4A left panel), and 8% in proximal tubule and Henle loop inner diameter value (Figure 4B and C, left panel).

DISCUSSION

All slides showed normal kidney histology. Under normal circumstances, histological structures including renal corpuscle, renal tubules, various types of vessels, in the cortical and medulla regions were identified under a bright field microscope. Magnification adjustment might require to gain greater details on the structures. Particular lesion or histological structures, might best be viewed in specific magnification, for example glomerular lesions it is usually observed at 400-1000x magnification while tubulointerstitial lesions is generally analysed at 100-400x magnification.¹¹

We obtained renal corpuscle means areas of $12.7\pm 2.9 \times 10^3 \mu\text{m}^2$ in QuPath and $12.5\pm 3.0 \times 10^3 \mu\text{m}^2$ from Fiji measurement. The glomerular areas were $7.8\pm 2.1 \times 10^3 \mu\text{m}^2$ and $7.8\pm 2.2 \times 10^3 \mu\text{m}^2$ for QuPath and Fiji respectively. The glomerulus has a round figure and approximately 200 μm diameter.^{12,13} The larger glomerular area was reported in patients with IgA nephropathy ($28.9 \times 10^3 \mu\text{m}^2$), Focal segmental glomerulosclerosis ($31.1 \times 10^3 \mu\text{m}^2$), Membranous glomerulonephritis ($27.9 \times 10^3 \mu\text{m}^2$),¹⁴ and in Secondary focal segmental glomerulosclerosis ($3.1 \times 10^4 \mu\text{m}^2$).¹⁵

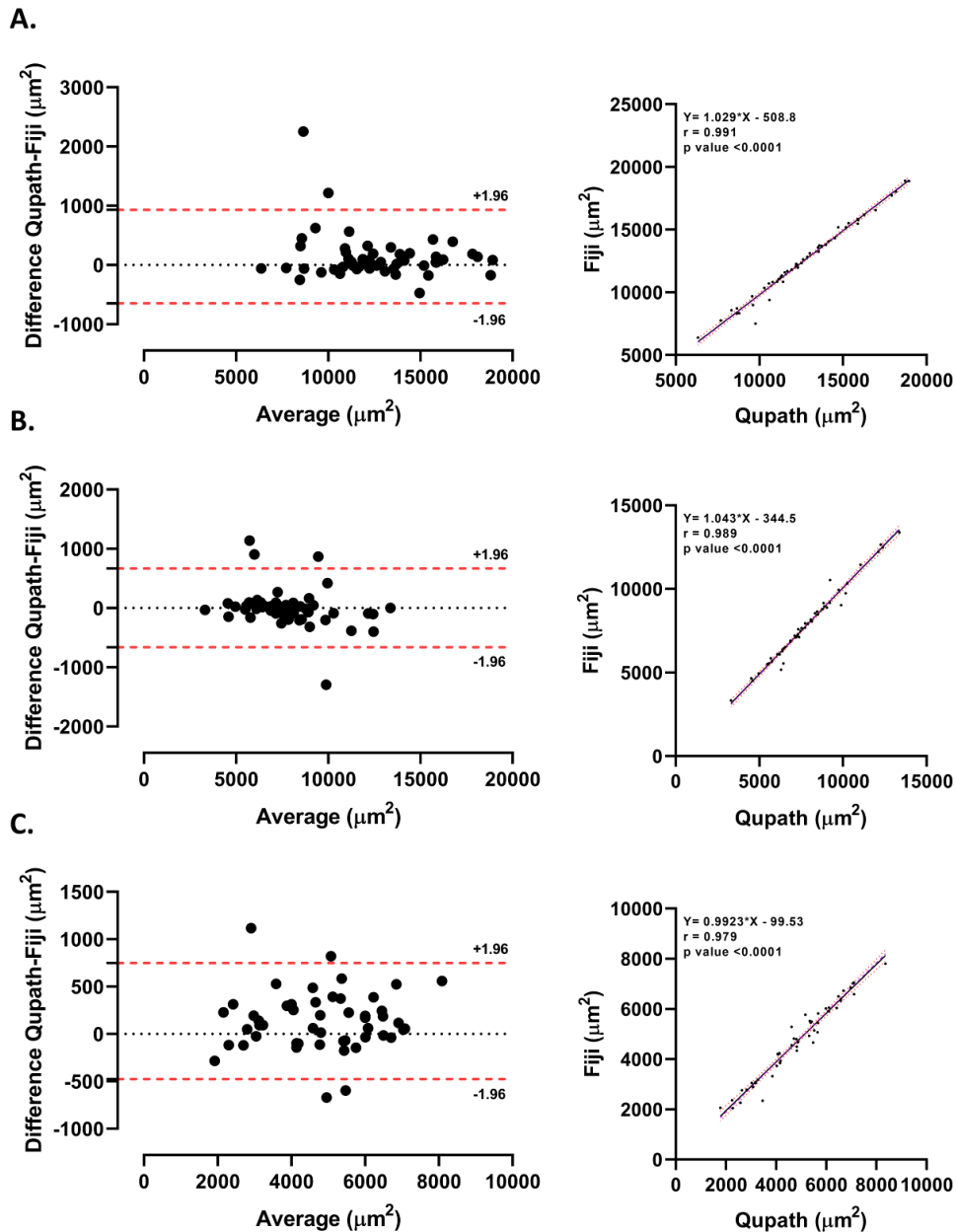


Figure 3. Bland-Altman plot (left panel) and Deming regression (right panel) between measurement results using QuPath and Fiji. (A) Renal corpuscle area (B) Glomerular area (C) Bowman space area. The red dashed line in Bland-Altman plot indicates the 95% of the upper and lower limits of agreements. In Deming regression panel, the black dot indicates data points, purple dash indicates Deming regression line, black line indicates simple regression line, and red dot indicates error bar for simple regression line.

The renal tubules varied in diameter and histological appearance. Based on our measurements, the proximal tubule's inner diameters ranged from 18.7 to 150.8 μm . Smaller inner diameters were observed in distal tubules (17.1-80.5 μm) and The Henle loop (15.5-69.6 μm). There are variations in lumen diameter according to the previous report, the mean diameter of the human tubular lumen was $39.6 \pm 1.8 \mu\text{m}$.¹⁶ The smaller mean diameter was reported at $29.5 \pm 9.2 \mu\text{m}$ within the 30 - 60 μm diameter range.¹⁷ Specified renal tubule segment, such as the proximal convoluted tubule was about 15 mm long and 55 μm in diameter.¹⁸ Contrary to popular belief, the renal convoluted tubules are elliptical rather than round due to the difference in mean length between the short

axis and the long axis. This issue should be considered when analyzing tubular area or diameter.¹⁹

The renal tubule diameters are often compared to other species in the animal model for kidney diseases. In mice, the normal proximal convoluted tubules' mean diameter was $37.4 \pm 0.5 \mu\text{m}$ (minimum diameter) and $44.0 \pm 0.7 \mu\text{m}$ (maximum diameter). For distal convoluted tubules, the mean minimum diameter was $32.2 \pm 0.6 \mu\text{m}$ and the mean maximum diameter was $40.2 \pm 0.9 \mu\text{m}$.¹⁹ Meanwhile the mean diameter for rat tubular lumen in the kidney cortex was rat $32.5 \pm 2.9 \mu\text{m}$.¹⁶ The external diameter of the Henle loop's thin section is about 12 μm . The near end collecting tube is 200 μm in diameter, while the small collecting tubule has a diameter of roughly 40 μm .²⁰

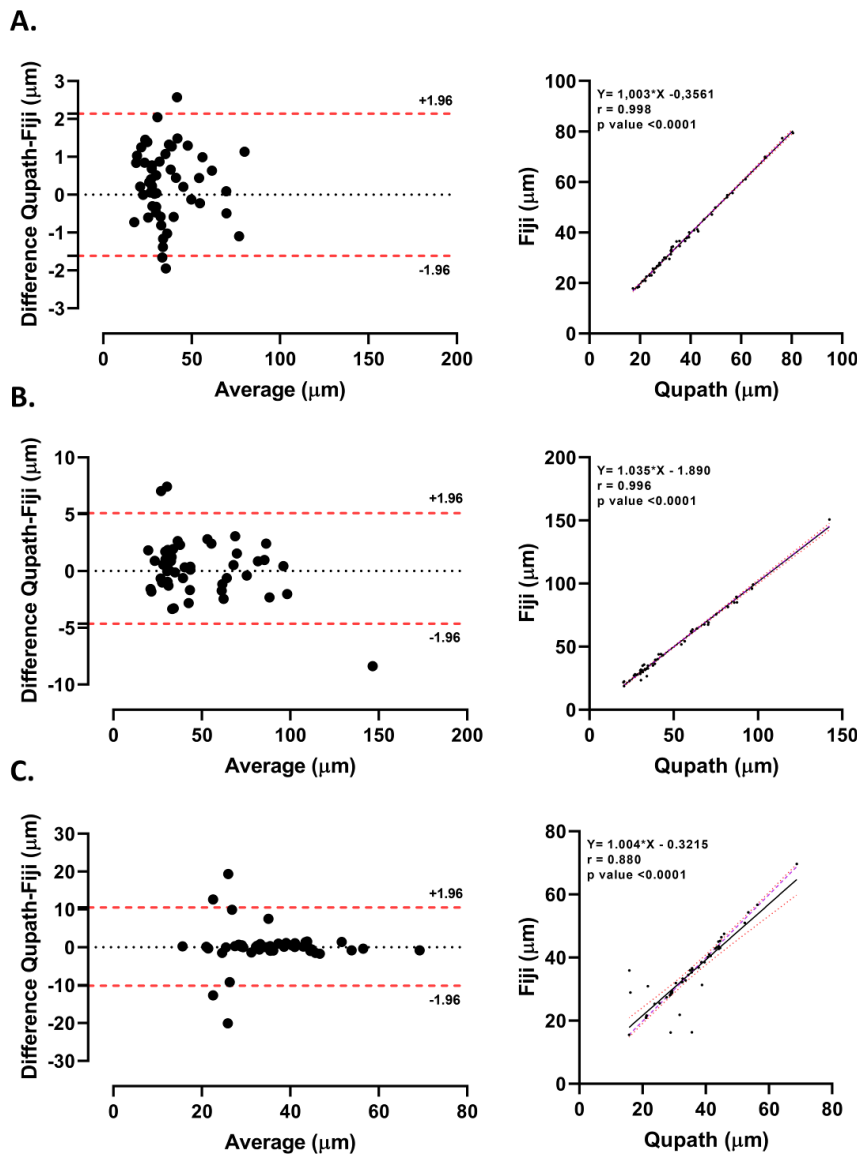


Figure 4. Bland-Altman plot (left panel) and Deming regression (right panel) between measurement results using QuPath and Fiji (renal tubules). (A) Distal tubule (B) Proximal tubule (C) Henle loop. The red dashed line indicates the 95% of the upper and lower limits of agreements. The red dashed line in Bland-Altman plot indicates the 95% of the upper and lower limits of agreements. In Deming regression panel, the black dot indicates data points, purple dash indicates Deming regression line, black line indicates simple regression line, and red dot indicates error bar for simple regression line.

In this study, we compare the measurement results of kidney microscopic structures using QuPath and Fiji. From our observation this two software were resulting comparable values. There was no significant difference in measurement results of renal corpuscle area, glomerular area, Bowman space area, luminal diameter of proximal tubules, distal tubules, and Henle loop between the compared software (p -value > 0.05). Further confirmational analysis supported the similarity between two measurement results. We analysed the quantification results using Deming regression and the Bland-Altman plot. Strong correlation and linearity from two measurements were also demonstrated in all observed kidney structures with Pearson's rho values greater than 0.995 for most structures except for the Henle loop ($r = 0.880$). We observed some values were outside the upper or lower limit of agreement. However, the majority of paired data lies within the lower and

upper limits of agreement of the Bland-Altman plot and only less than 10% off-limit values. The evidence supports that both measurement values were identical.

Based on our experience, both QuPath and Fiji are user-friendly and reliable for renal histomorphometric analysis. However, our team found that QuPath provides better workspace visualization compared to Fiji. Which affects our navigation performance or response while working on the project. In addition, annotating, object measurement, and project management were more convenient to perform in QuPath.

We note limitations in our study. Since WSI analysis is not feasible in our team setting. We were not able to compare the measurement results of both software with the WSI result as the "gold standard".

In conclusion, the measurement result of kidney microstructures using QuPath and Fiji were identical. The researcher can select QuPath or Fiji for kidney

histomorphometry and expect relatively similar measurement results. For researchers who are constrained to conducting research using unbiased stereology or WSI, the availability of reliable and user-friendly software can aid in carrying out histomorphometry analysis.

ACKNOWLEDGEMENT

The author would like to acknowledge the Lembaga Penelitian dan Pengabdian pada Masyarakat (LPPM) of Universitas Muhammadiyah Purwokerto for funding this research.

REFERENCES

- Klopfleisch R. Multiparametric and semiquantitative scoring systems for the evaluation of mouse model histopathology--a systematic review. *BMC Vet Res.* 2013;9:123. doi: 10.1186/1746-6148-9-123.
- Meyerholz DK, Beck AP. Fundamental Concepts for Semiquantitative Tissue Scoring in Translational Research. *ILAR J.* 2018;59(1):13-7. doi: 10.1093/ilar/ily025.
- Rueden CT, Schindelin J, Hiner MC, DeZonia BE, Walter AE, Arena ET, et al. ImageJ2: ImageJ for the next generation of scientific image data. *BMC Bioinformatics.* 2017;18(1):1-26. doi: 10.1186/s12859-017-1934-z.
- Schindelin J, Arganda-Carreras I, Frise E, Kaynig V, Longair M, Pietzsch T, et al. Fiji: an open-source platform for biological-image analysis. *Nat Methods.* 2012;9(7):676-82. doi: 10.1038/nmeth.2019.
- Jones TR, Kang IH, Wheeler DB, Lindquist RA, Papallo A, Sabatini DM, et al. CellProfiler Analyst: data exploration and analysis software for complex image-based screens. *BMC Bioinformatics.* 2008;9(1):482. doi: 10.1186/1471-2105-9-482.
- Piccinini F, Balassa T, Szkalicity A, Molnar C, Paavolainen L, Kujala K, et al. Advanced Cell Classifier: User-Friendly Machine-Learning-Based Software for Discovering Phenotypes in High-Content Imaging Data. *Cell Syst.* 2017;4(6):651-5. doi: 10.1016/j.cels.2017.05.012.
- Berg S, Kutra D, Kroeger T, Straehle CN, Kausler BX, Haubold C, et al. ilastik: interactive machine learning for (bio)image analysis. *Nat Methods.* 2019;16(12):1226-32. doi: 10.1038/s41592-019-0582-9.
- Sommer C, Hoefler R, Samwer M, Gerlich DW. A deep learning and novelty detection framework for rapid phenotyping in high-content screening. *Mol Biol Cell.* 2017;28(23):3428-36. doi: 10.1091/mbc.E17-05-0333.
- Farahani N, Parwani A, Pantanowitz L. Whole slide imaging in pathology: advantages, limitations, and emerging perspectives. *Pathol Lab Med Int.* 2015;7:23-33. doi: 10.2147/PLMI.S59826.
- Kumar N, Gupta R, Gupta S. Whole Slide Imaging (WSI) in Pathology: Current Perspectives and Future Directions. *J Digit Imaging.* 2020;33(4):1034-40. doi: 10.1007/s10278-020-00351-z.
- Rangan GK, Tesch GH. Quantification of renal pathology by image analysis (Methods in Renal Research). *Nephrology.* 2007;12(6):553-8. doi: 10.1111/j.1440-1797.2007.00855.x.
- Cho K-O, Lee SH, Jang H-J. Feasibility of fully automated classification of whole slide images based on deep learning. *Korean J Physiol Pharmacol.* 2019;24(1):89-99. doi: 10.4196/kjpp.2020.24.1.89.
- Samuel T, Hoy WE, Douglas-Denton R, Hughson MD, Bertram JF. Applicability of the glomerular size distribution coefficient in assessing human glomerular volume: the Weibel and Gomez method revisited. *J Anat.* 2007;210(5):578-82. doi: 10.1111/j.1469-7580.2007.00715.x.
- Turgut D. Measurement of glomerular area in primary glomerular diseases with a digital pathology software. *Journal of clinical and experimental investigations.* 2021;48(1):9-16. doi: 10.5798/dicletip.887368.
- Zamami R, Kohagura K, Kinjyo K, Nakamura T, Kinjo T, Yamazato M, et al. The Association between Glomerular Diameter and Secondary Focal Segmental Glomerulosclerosis in Chronic Kidney Disease. *Kidney Blood Press Res.* 2021;46(4):433-40. doi: 10.1159/000515528.
- Morozov D, Parvin N, Charlton JR, Bennett KM. Mapping kidney tubule diameter ex vivo by diffusion MRI. *Am J Physiol Renal Physiol.* 2021;320(5):F934-F46. doi: 10.1152/ajprenal.00369.2020.
- Li Q, Onozato ML, Andrews PM, Chen CW, Paek A, Naphas R, et al. Automated quantification of microstructural dimensions of the human kidney using optical coherence tomography (OCT). *Opt Express.* 2009;17(18):16000-16. doi: 10.1364/oe.17.016000.
- Barrett KE, Barman SM, Yuan JXJ, Brooks H. Ganong's review of medical physiology. 26th ed. ed. New York, N.Y: McGraw-Hill Education LLC.; 2019.
- Ortega-Martinez M, Gutierrez-Davila V, Gutierrez-Arenas E, Niderhauser-Garcia A, Cerda-Flores RM, Jaramillo-Rangel G. The Convolute Tubules of the Nephron Must Be Considered Elliptical, and Not Circular, in Stereological Studies of the Kidney. *Kidney Blood Press Res.* 2021;46(2):229-35. doi: 10.1159/000515051.
- Alicelebić S. Proximal convolute tubules of the rats kidney--a stereological analysis. *Bosn J Basic Med Sci.* 2003;3(1):36-9. doi: 10.17305/bjbms.2003.3568.